Supplementary information

The crystal structure of Dph2 in complex with elongation factor 2 reveals the structural basis for the first step of diphthamide biosynthesis

Michael K. Fenwick, [1] Min Dong,[1] Hening Lin[1,2] and Steven E. Ealick,[1,*]

[1]Department of Chemistry and Chemical Biology, [2]Howard Hughes Medical Institute, Cornell University, Ithaca, New York, 14853.

[*]To whom correspondence should be addressed: see3@cornell.edu

Table S1

Codon optimized *dph2*
CATATGAGCATGTATAACATGGACCTGGATAAAGTGATTCGTAAGATTAACAAAAAGGGTGCGCGTACCGTTGGCCTGCAATTCCCGGA GGGCCTGAAAATGCAGGCGGTGAAGATCGCGAAAGCGATTGAGAGCCAAACCCCGGCGACCGTGATCATTAGCGGTGACCCGTGCTTTG GTGCGTGCGACGTTAGCGATTACAAGATGAAAGGTAGCGTGGATCTGATCGTTCACTACGGCCACACCCCGCTGCCGCTGAAATATGAG GTGCCGACCCTGTTCATCGAAGCGTTTAGCAACATTGACGTTAAGAAAGATCTGGAGAAGTGCCTGGAGAAACTGGAAGACTACAGCAA GATCGCGCTGGTTACCACCACCCAGCACCTGCACCTGCTGAACGAAATTAAGGACTATCTGGAGGATAACGGTAAAGAAGTGGTTCTGG GCAGCAGCAAGAACACCAAGAAAGGTCAAGTGCTGGGCTGCAACTTCAGCAGCATCAAAAACCTGGACGCGGAAGTGTACCTGTTCATC GGTAGCGGCAACTTTCACCCGCTGGGTATTTACCTGTTTACCAAGAGCCCGGTGCTGGCGCTGGATCCGTATAACAGCGAAATCCGTGA CATTAGCGCGTTCGCGGATCGTATCCTGCGTATTCGTTTTGCGCGTATTACCAAGGCGCGTGAGGCGGAAAAATGGGGTATCATTGTTA GCAGCAAAGAGGGCCAGTACCGTATGAAGCTGGCGAAAGAAATCAAGAAAATTCTGGAGGACAACAAGATGGAAGCGTACATCATTATG GCGGACAACATCAACCCGGATATTCTGCTGCCGTATATGGAACTGGATGCGTTTGTGGTTAGCGCGTGCCCGCGTATCGCGATTGACGA TAGCCAGATGTATAAGAAACCGCTGCTGACCCCGCAAGAGCTGGAAATCGTGCTGAACAAACGCCAATGGGAGAACTACCAACTGGACG AAATCCTGTTTCACGAACGCTACAAGTAACTCGAG
Codon optimized *his6tag-ef-2*
CCATGGGCAGCGATAAGATCCACCACCACCACCACCACAGCAGCGGCGAGAACCTGTATTTTCAAGGCAGCGGTATGAGCCGTCGTGAG AAGATGATCGCGAAGATTAAAGACCTGATGTATAAACCGGATAGCATCCGTAACATCGGTATTTGCGCGCACATTGACCACGGCAAGAC CACCCTGAGCGATAACCTGCTGGCGGGTGCGGGCATGATCAGCGAGGAACTGGCGGGTGACCAGCGTTTCCTGGACTTTGATGAGCAGG AACAAGCGCGTGGCATCACCATTGATGCGGCGAACGTGAGCATGGTTCACAACTACAAAGACGAGGAATATCTGATCAACCTGATTGAT ACCCCGGGTCACGTGGACTTCGGTGGCGATGTTACCCGTGCGATGCGTGCGGTGGATGGTGCGGTGGTTGTGGTTTGCGCGGTTGAAGG CATTATGCCGCAGACCGAAACCGTGCTGCGTCAAGCGCTGAAAGAGAACGTGAAGCCGGTTCTGTTCATCAACAAGGTGGACCGTCTGA TTAACGAGCTGAAACTGGAACCGGAGGAACTGCAGAAGCGTTTCATCAACATCTACATGGAAGCGAACAAACTGATCAAGAACATGGCG CCGGAGGATAAGAAAGAGGAATGGGCGGTGGACTTCACCGATGGTAGCGTTGCGTTTGGCAGCGCGTATCACAACTGGGCGATTAACGT GCCGATGATGCAAGAAACCGGTGTTAACTTCAAAGACATCATTGATTACTGCAACGACGATAAGCAGAAAGAGCTGGCGCAAAAGGTGC CGCTGAGCGAAGTTCTGCTGGGCATGGTGGTTGAGCACCTGCCGAGCCCGAAAGTGAGCCAGGAGTACCGTGTTCCGAACATCTGGGAG GGTGACATTGAAAGCCCGGCGGGTCAGGGTATGATTACCACCAGCCCGGATGGTCCGCTGGCGGTGATGGTTACCAACGTGAGCGTTGA TAAGCACGCGGGTGAAATCGCGACCGGCCGTGTGTACGGTGGCAGCATTGAGAAAGGTACCGAAGTGTATCTGGTTGGCAGCCACAGCA AGAGCCGTGTTCAGCAAGTGGGTGTTTATTTCGGCCCGGAGCGTGTGAACACCGATGCGGTTCCGGCGGGTAACATCGTGTATGTTGCG GGTGCGAAAGGTGCGATTGCGGGCGAAACCATTTGCAGCCCGGAGGACAAGATCAAAGAGTTTGAAGGTCTGGATCACATTAGCGAACC GGTGGTTACCGTGGCGGTTGAGGCGAAAAACACCAAGGACCTGCCGAAGCTGATTGAAGTGCTGCGTCAGGTTGCGAAAGAAGATCCGA CCATCAAGGTTGAGATTAACGAGGAAACCGGTGAACACCTGGTTAGCGGTATGGGCGAGCTGCACCTGGAAGTGATCAGCTATCGTATT AAGGACAAAGGCGTTGAGATCCAAACCAGCGAACCGATTGTGGTTTACCGTGAAACCGTGAGCCAGCTGAGCCCGCAAGTTGAGGGTAA AAGCCCGAACAAGCACAACCGTTTCTACATCACCGTGGAGCCGCTGGAGGACGAACTGTTTAAAGCGCTGCAGGAAGGTAAACTGAAAG

AAGGTAAAGTGAAAGGCAAGGAGAGCGCGAACGACTTCATGGAATACGGCCTGGATAAAGAGGAAGCGCGTAAAGTGTGGGATGTTTAT

AACCGTAGCGTGTTTATCAACGCGACCCGTGGTATTCAATACCTGGACGAGGTTAAGGAACTGCTGATCGAGGGTTTCGAAAGCGCGCT

GAACGATGGCCCGCTGGCGAAAGAAATTGCGATGGGTCTGAAATTTAAGCTGCACGACGCGAAGCTGCACGAGGATGCGGTTCATCGTG

GTCCGGCGCAGGTTCTGCCGGCGATCCGTAACGCGATTTATGCGAGCATGATGAGCGCGGGTCCGACCCTGCTGGAACCGATGCAGAAA

GTGTTCATCAACACCCCGCAAGACTACATGGGTCCGTGCACCCGTGAGATCCAGAACCGTCGTGGCCAAATTGTTGACATGGGTCAGGA

AGGTGATATGGCGACCATCGAAAGCAAGGTGCCGGTTGCGGAGATGTTCGGTTTTGCGGGCGATATTCGTAGCGCGGCGGAAGGTCGTT

GCCTGTGGAGCACCGAGATGAGCGGCTTTGAACGTCTGCCGCGTGAGATGCAGAACCAAATCGTGAAAGAGATTCGTCAACGCAAAGGT

CTGAGCCCGGAGCCGTATGGCCCGGAACACTATGTGGGTTAAGCGGCCGC

Supplementary figure legends

Figure S1. Electron density of the two molecules of *Ms*EF-2 in the asymmetric unit. (A) Ordered molecule of *Ms*EF-2. (B) Domains III-V of the disordered molecule of *Ms*EF-2. Protein chains are shown as Cα atom traces. (C) F_o-F_c electron density of the turn containing His597. (D) Sharpened 2F_o-F_c electron density[1, 2] of the turn containing His597. The electron density maps in panels C and D were generated prior to introducing the turn into the model.

Figure S2. Electron density of the two molecules of *Ms*Dph2 in the asymmetric unit. (A,B) 2F_o-F_c composite omit maps.[3, 4] The map regions are contoured at two and seven times the RMSD of the maps in panels A and B, respectively. (C) Unassigned F_o-F_c electron density in the active site of *Ms*Dph2A. The conformation of SAM bound to *Cmn*Dph2 (PDB entry 6BXM)[5] was rigidly fit to show that the electron density has a shape resembling SAM, SAM cleavage products, or structural analogs of these molecules. Protein chains are shown as Cα atom traces and SAM and the [4Fe-4S] clusters as balls and sticks.

Figure S3. Surface representation of the domain IV-*Ms*Dph2A interface. Two views are shown differing by a rotation about the x axis by 90 degrees and about the z axis by 180 degrees. MTA (spheres with carbon atoms colored green) is placed based on a superimposition of the isolated structure of *Ms*Dph2-MTA onto *Ms*Dph2A.

Figure S4. Difference distance matrices[6] indicating structural changes in main chains of *Ms*EF-2 and *Ms*Dph2 upon complex formation. (A) Structural changes in main chain of EF-2. Difference distances (reported in Angstroms) were computed for Cα atoms of domain IV of *Ms*EF-2 bound to *Ms*Dph2A and domain IV of *Ph*EF-2 (PDB entry 5H7J).[7]

(B) Structural changes in main chain of Dph2. Difference distances were computed for Cα atoms of *Ms*Dph2A and a protomer of isolated *Ms*Dph2-MTA.

Figure S5. Multiple amino acid sequence alignment of twenty archaebacterial Dph2 orthologs. Alignments were produced using MUSCLE[8] and illustrated using ESPript.[9] The species and associated sequence accession codes are *Methanobrevibacter smithii* ATCC 35061 (ABQ87563.1), *Candidatus Methanoperedens nitroreducens* (WP_048090324.1), *Pyrococcus horikoshii* (WP_010885188.1), *Methanotorris formicicus* (WP_007044710.1), *Methanococcus voltae* A3 (ADI37130.1), *Thaumarchaeota archaeon* (PHY04318.1), *Nitrosarchaeum koreense* (WP_007551417.1); *Methanothermobacter marburgensis str. Marburg* (ADL59274.1); *Methanosphaera stadtmanae* (RAP02414.1), *Methanosarcina barkeri* (WP_011306625.1); *Methanolobus profundi* (WP_091934691.1); *Methanococcoides methylutens* (KGK98218.1); *Methanosaeta harundinacea* 6Ac (AET64119.1), *Candidatus Methanomethylophilus alvus* (WP_122892392.1); *Pyrococcus abyssi* (WP_010868245.1); *Halorubrum vacuolatum* (WP_089383146.1); *Saccharolobus solfataricus* (WP_009990583.1); *Natrinema altunense* (WP_007108593.1); *Acidiplasma* (WP_048102160.1); *Thermofilum uzonense* (WP_052884265.1).

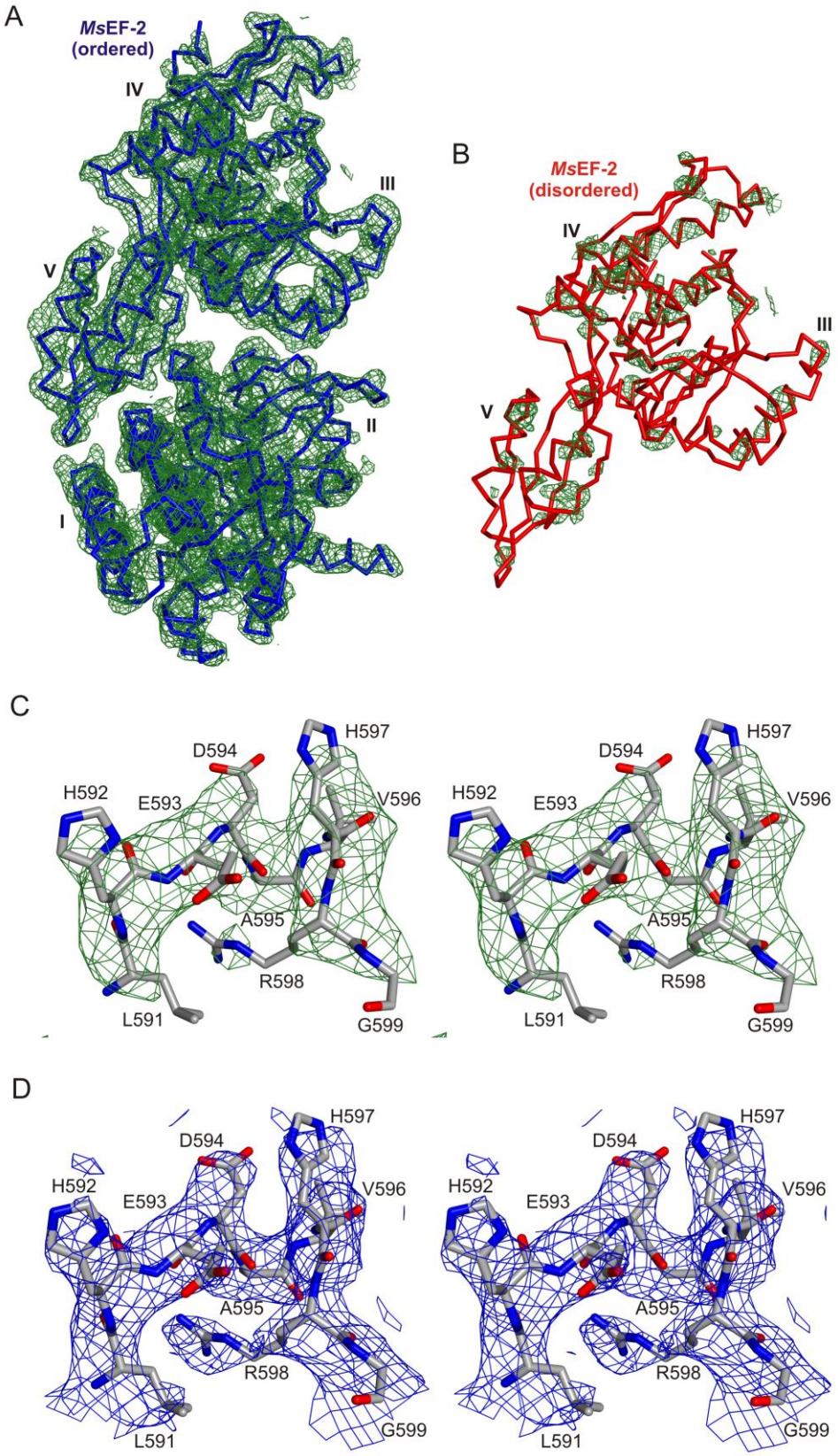
A
MsEF-2
(ordered)
IV
III
V
II
I
B
MsEF-2
(disordered)
IV
III
V
C
H597
D594
H592
E593
V596
A595
R598
L591
G599
H597
D594
H592
E593
V596
A595
R598
L591
G599
D
H597
D594
H592
E593
V596
A595
R598
L591
G599
H597
D594
H592
E593
V596
A595
R598
L591
G599

Figure S1

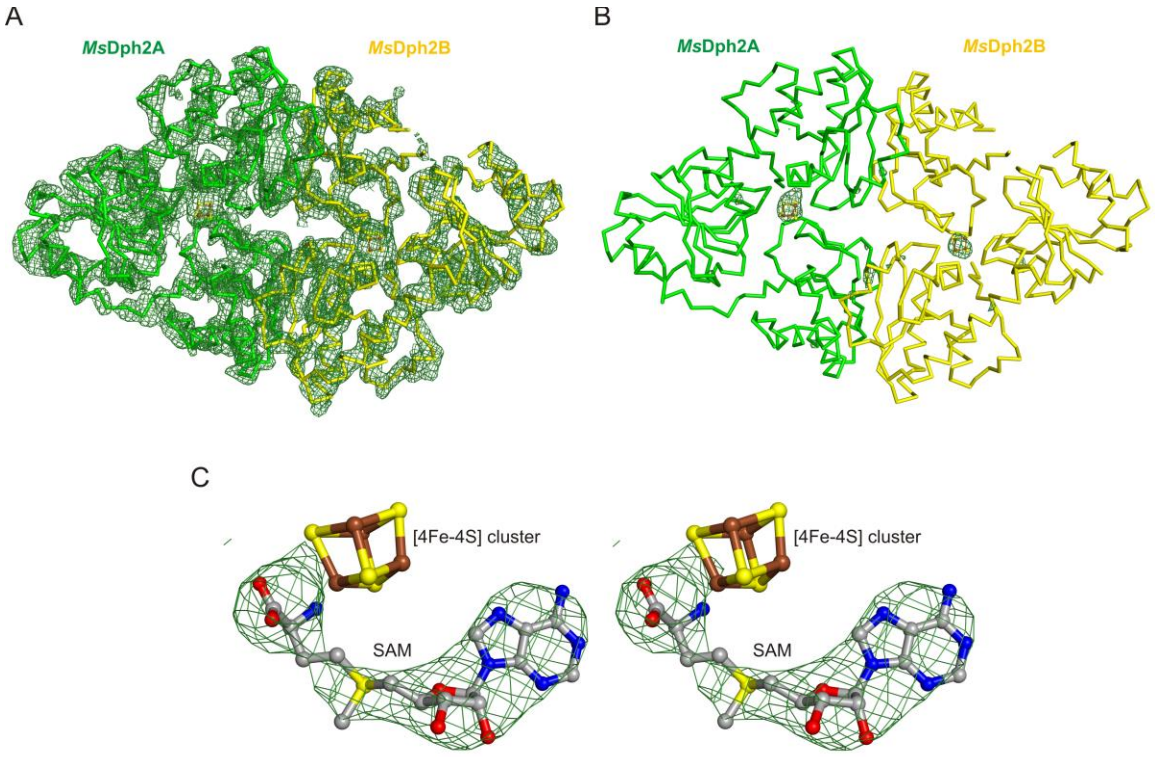
A
MsDph2A
MsDph2B
B
MsDph2A
MsDph2B
C
[4Fe-4S] cluster
SAM
[4Fe-4S] cluster
SAM

Figure S2

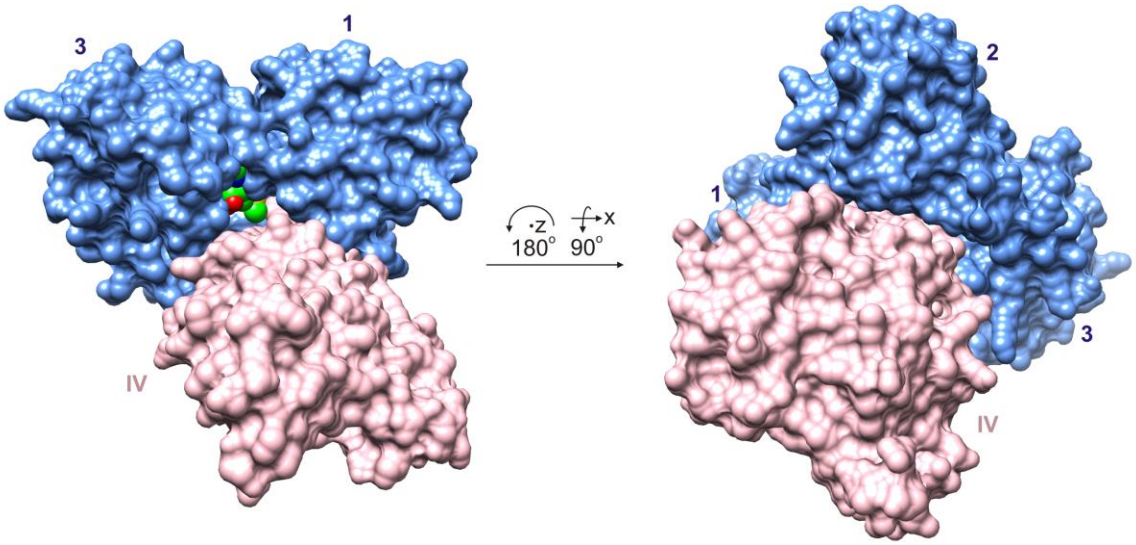

Figure S3

A

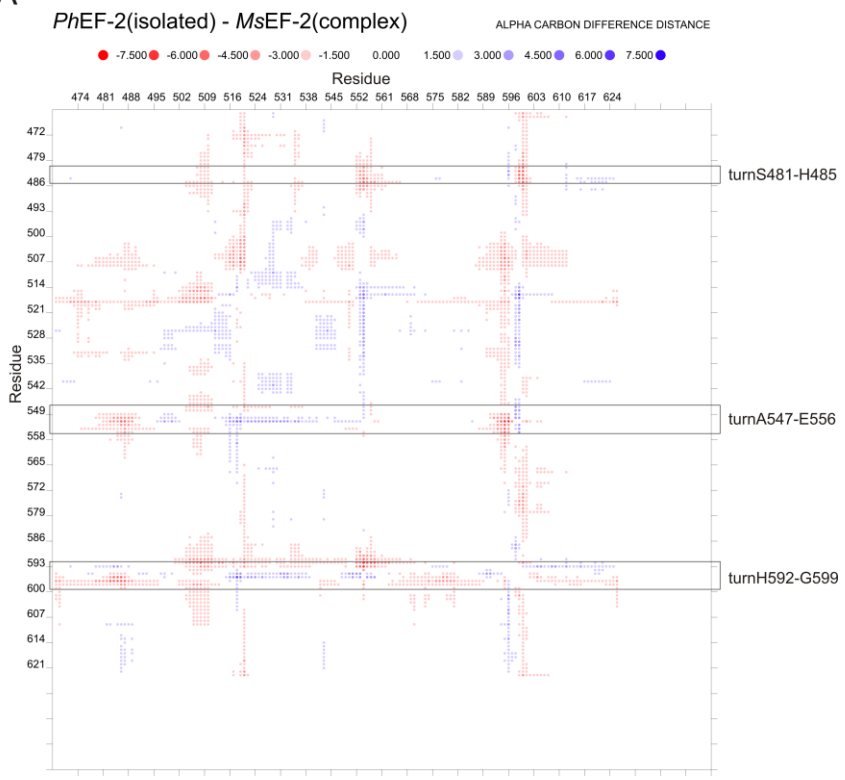
*Ph*EF-2(isolated) - *Ms*EF-2(complex)
ALPHA CARBON DIFFERENCE DISTANCE
-7.500 -6.000 -4.500 -3.000 -1.500 0.000 1.500 3.000 4.500 6.000 7.500
Residue
474 481 488 495 502 509 516 524 531 538 545 552 561 568 575 582 589 596 603 610 617 624
Residue
472 479 486 493 500 507 514 521 528 535 542 549 558 565 572 579 586 593 600 607 614 621
turnS481-H485
turnA547-E556
turnH592-G599

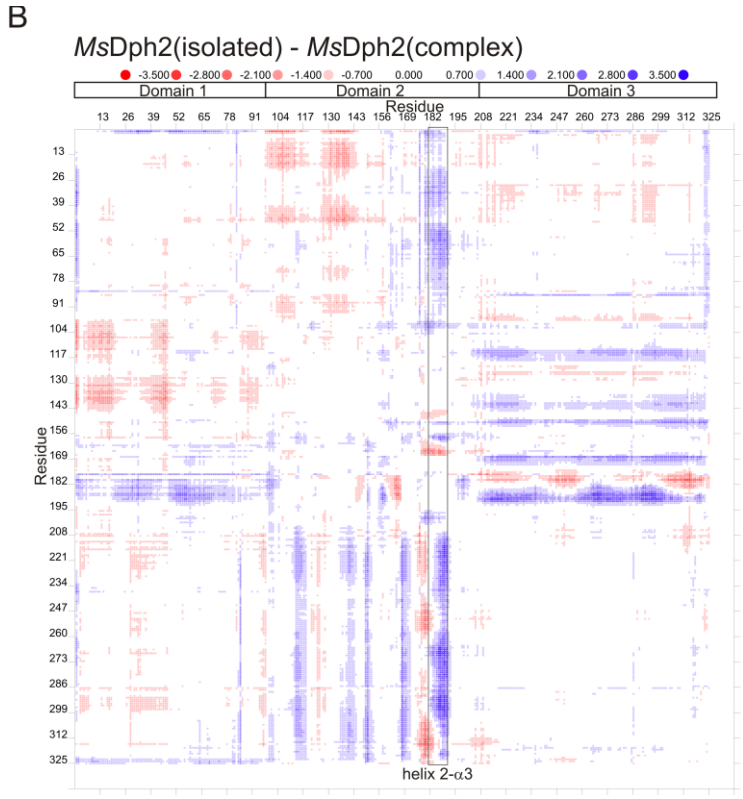
B
MsDph2(isolated) - MsDph2(complex)
-3.500 -2.800 -2.100 -1.400 -0.700 0.000 0.700 1.400 2.100 2.800 3.500
Domain 1
Domain 2
Domain 3
Residue
13 26 39 52 65 78 91 104 117 130 143 156 169 182 195 208 221 234 247 260 273 286 299 312 325
Residue
helix 2-α3

Figure S4

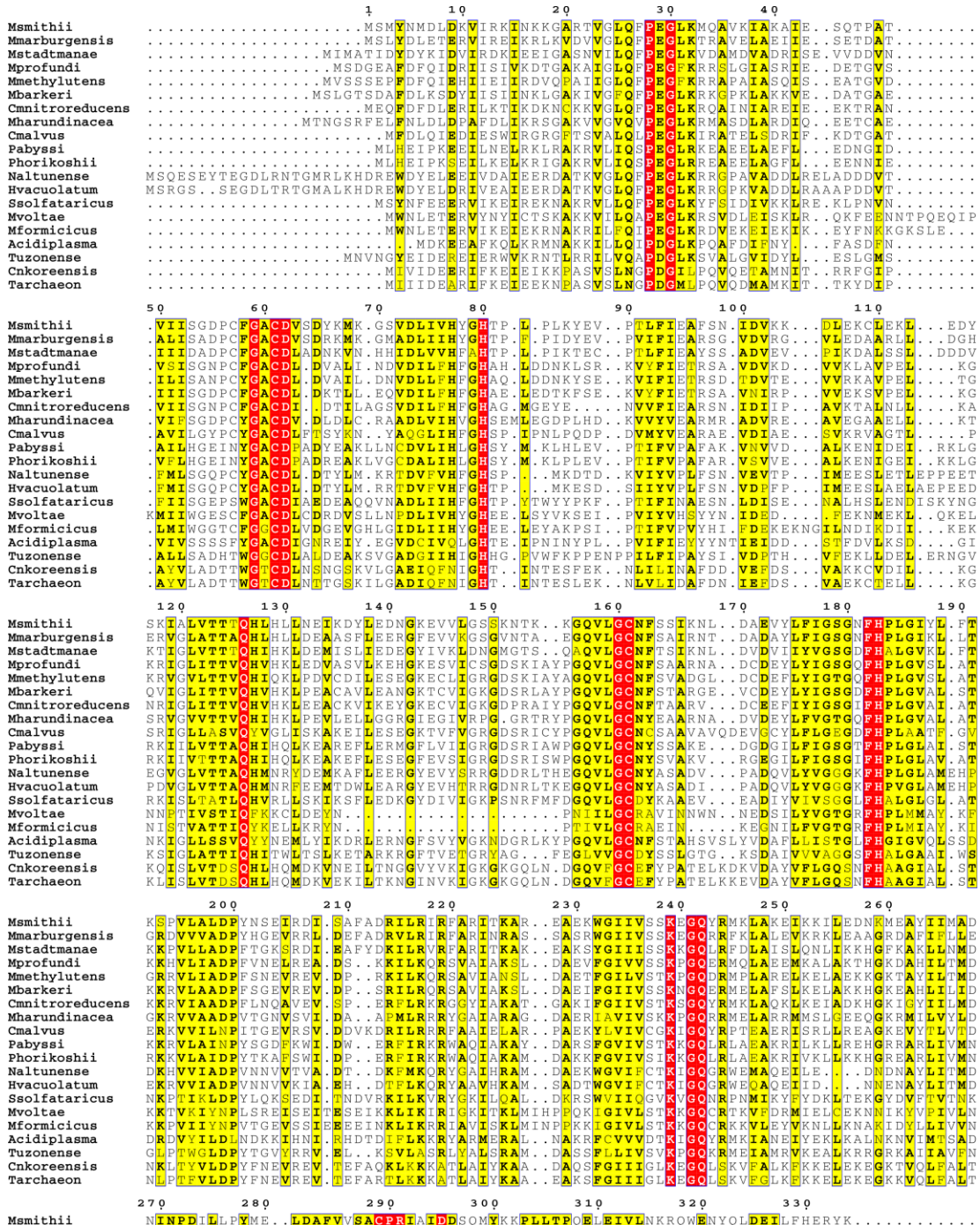
Msmithii
Mmarburgensis
Mstadtmanae
Mprofundi
Mmethylutens
Mbarkeri
Cmnitroreducens
Mharundinacea
Cmalvus
Pabyssi
Phorikoshii
Naltunense
Hvacuolatum
Ssolfataricus
Mvoltae
Mformicicus
Acidiplasma
Tuzonense
Cnkoreensis
Tarchaeon

Figure S5

References

(1) Emsley, P., Lohkamp, B., Scott, W. G., and Cowtan, K. (2010) Features and development of Coot, *Acta Cryst. D66*, 486-501.

(2) Terwilliger, T. C., Sobolev, O. V., Afonine, P. V., and Adams, P. D. (2018) Automated map sharpening by maximization of detail and connectivity, *Acta Cryst. D74*, 545-559.

(3) Adams, P. D., Afonine, P. V., Bunkoczi, G., Chen, V. B., Echols, N., Headd, J. J., Hung, L. W., Jain, S., Kapral, G. J., Grosse Kunstleve, R. W., McCoy, A. J., Moriarty, N. W., Oeffner, R. D., Read, R. J., Richardson, D. C., Richardson, J. S., Terwilliger, T. C., and Zwart, P. H. (2011) The Phenix software for automated determination of macromolecular structures, *Methods 55*, 94-106.

(4) Afonine, P. V., Moriarty, N. W., Mustyakimov, M., Sobolev, O. V., Terwilliger, T. C., Turk, D., Urzhumtsev, A., and Adams, P. D. (2015) FEM: feature-enhanced map, *Acta Cryst. D71*, 646-666.

(5) Dong, M., Kathiresan, V., Fenwick, M. K., Torelli, A. T., Zhang, Y., Caranto, J. D., Dzikovski, B., Sharma, A., Lancaster, K. M., Freed, J. H., Ealick, S. E., Hoffman, B. M., and Lin, H. (2018) Organometallic and radical intermediates reveal mechanism of diphthamide biosynthesis, *Science 359*, 1247-1250.

(6) Richards, F. M., and Kundrot, C. E. (1988) Identification of structural motifs from protein coordinate data: secondary structure and first-level supersecondary structure, *Proteins 3*, 71-84.

(7) Tanzawa, T., Kato, K., Girodat, D., Ose, T., Kumakura, Y., Wieden, H. J., Uchiumi, T., Tanaka, I., and Yao, M. (2018) The C-terminal helix of ribosomal P stalk recognizes a hydrophobic groove of elongation factor 2 in a novel fashion,

Nucleic Acids Res. 46, 3232-3244.

(8) Edgar, R. C. (2004) MUSCLE: multiple sequence alignment with high accuracy and high throughput, *Nucleic Acids Res. 32*, 1792-1797.

(9) Robert, X., and Gouet, P. (2014) Deciphering key features in protein structures with the new ENDscript server, *Nucleic Acids Res. 42*, W320-324.